<div align="center">**Fracture**</div>

1 Williams expansion

This section is taken from Eran's lecture notes

Consider a linear elastic solid under quasi-static conditions, for which we have

$$\nabla^2 \nabla^2 \chi(r,\theta) = \left(\partial_{rr} + r^{-1}\partial_r + r^{-2}\partial_{\theta\theta}\right)^2 \chi(r,\theta) = 0 \ . \tag{1}$$

where $\chi(r,\theta)$ is the Airy stress potential. Let us look for a solution of the form $\chi(r,\theta) = r^{\lambda+2} f(\theta)$ (you already know from previous discussions that there are more solutions, e.g. $\log r$). Operating with ∇^2 on this Ansatz, we obtain

$$\left(\partial_{rr} + r^{-1}\partial_r + r^{-2}\partial_{\theta\theta}\right) r^{\lambda+2} f(\theta) = r^{\lambda}\left[(\lambda+2)^2 + \frac{d^2}{d\theta^2}\right] f(\theta) \equiv r^{\lambda} g(\theta) \ . \tag{2}$$

Operating with ∇^2 again yields

$$\left(\partial_{rr} + r^{-1}\partial_r + r^{-2}\partial_{\theta\theta}\right) r^{\lambda} g(\theta) = r^{\lambda-2}\left[\lambda^2 + \frac{d^2}{d\theta^2}\right] g(\theta) = 0 \ , \tag{3}$$

and therefore we end up with the following ordinary differential equation

$$\left[\lambda^2 + \frac{d^2}{d\theta^2}\right]\left[(\lambda+2)^2 + \frac{d^2}{d\theta^2}\right] f(\theta) = 0 \ . \tag{4}$$

Assume then a solution of the form $f(\theta) = e^{\alpha\theta}$, which leads to the following algebraic equation

$$\left[\lambda^2 + \alpha^2\right]\left[(\lambda+2)^2 + \alpha^2\right] = 0 \ . \tag{5}$$

The solution is

$$\alpha_{1,2} = \pm i\lambda \quad \alpha_{1,2} = \pm i(\lambda+2) \ , \tag{6}$$

therefore

$$f(\theta) = a\cos(\lambda\theta) + b\cos[(\lambda+2)\theta] + c\sin(\lambda\theta) + d\sin[(\lambda+2)\theta] \ . \tag{7}$$

To determine the parameters we need to introduce a crack. Consider then a straight mode I crack where (r,θ) represents a coordinate system attached to the tip and $\theta = 0$ points in the direction of the tangent to the crack tip. Symmetry alone, $f(\theta) = f(-\theta)$, implies $c = d = 0$. As we explained above, a crack is introduced mathematically as traction-free boundary conditions of the form

$$\sigma_{\theta\theta}(r,\theta{=}\pm\pi) = \partial_{rr}\chi(r,\theta{=}\pm\pi) = 0, \quad \sigma_{r\theta}(r,\theta{=}\pm\pi) = -\partial_r\left(r^{-1}\partial_\theta\chi(r,\theta{=}\pm\pi)\right) = 0 \ . \tag{8}$$

Using $\chi(r,\theta) = r^{\lambda+2}\left(a\cos(\lambda\theta) + b\cos[(\lambda+2)\theta]\right)$, we obtain

$$\sigma_{\theta\theta}(r,\theta) = (\lambda+2)(\lambda+1)r^\lambda\left(a\cos(\lambda\theta) + b\cos[(\lambda+2)\theta]\right) , \tag{9}$$

$$\sigma_{r\theta}(r,\theta) = (\lambda+1)r^\lambda\left(a\lambda\sin(\lambda\theta) + (\lambda+2)b\sin[(\lambda+2)\theta]\right) . \tag{10}$$

Applying the boundary conditions, we obtain

$$(a+b)\cos(\lambda\pi) = 0 , \tag{11}$$

$$[a\lambda + b(\lambda+2)]\sin(\lambda\pi) = 0 . \tag{12}$$

Denoting $n = 0, \pm1, \pm2, ...$, the solution reads

$$\lambda = n \qquad \Longrightarrow \qquad b = -a , \tag{13}$$

$$\lambda = \frac{2n+1}{2} \qquad \Longrightarrow \qquad b = -\frac{a\lambda}{\lambda+2} . \tag{14}$$

We therefore end up with the Williams eigenfunctions expansion

$$\sigma_{ij}(r,\theta) = \sum_{m=-\infty}^{m=\infty} a_m r^{m/2} f_{ij}^{(m)}(\theta) , \tag{15}$$

where $f_{ij}^{(m)}(\theta)$ are explicitly expressed in terms of trigonometric functions as above. An immediate striking feature here is that the expansion contains half-integer powers. These emerge from the fact that a crack introduces a discontinuity in the fields, i.e. a crack is regarded as a mathematical branch cut.

What can we say about $\{a_m\}$? How can one calculate them? It is crucial to understand that we *did not* consider the outer boundary conditions of the problem, i.e. we essentially performed a crack tip asymptotic expansion, without even formulating the global boundary-value problem. $\{a_m\}$ are determined from the solution of each specific global boundary-value problem, which in general cannot be done analytically. The Williams expansion in Eq. (15) is therefore universal, independent of the external geometry and boundary conditions. The asymptotic expansion of course has a finite radius of convergence typically determined by some geometric properties of the crack, e.g. length for straight cracks or curvature for non-straight ones (note that we imposed the boundary conditions at $\theta = \pm\pi$, assuming that on the scale of interest any path curvature can be neglected).

2 Universal singular crack tip fields

The next question we would like to ask ourselves is whether all m's in the Williams expansion in Eq. (15) are physically acceptable? The point is the following: all terms with $m < -1$ will lead to *unbounded* linear elastic strain energy in the $r \to 0$ limit. To see this, recall that in a linear theory we have $\boldsymbol{\varepsilon} \sim \boldsymbol{\sigma} \sim r^{m/2}$ and hence the strain energy density scales as $\frac{1}{2}\sigma_{ij}\varepsilon_{ij} \sim r^m$. Therefore, the energy per unit thickness reads $\int \frac{1}{2}\sigma_{ij}\varepsilon_{ij}\, r\, dr\, d\theta \sim \int r^{m+1} dr$. It diverges in the $r \to 0$ limit for $m < -1$ (more precisely, we

are interested in the energy flux into the tip region when the crack advances incrementally, which in fact does not involve integration over r, as will be discussed below). We should therefore rewrite Eq. (15) as

$$\sigma_{ij}(r,\theta) = \sum_{m=-1}^{m=\infty} a_m r^{m/2} f_{ij}^{(m)}(\theta) \; . \qquad (16)$$

The above discussion has serious implications. As we have included the $m = -1$ term in the expansion, it seems as if we allow the stress tensor to diverge in the $r \to 0$ limit as long as it results in an integrable elastic energy. This divergence is precisely the one we discussed in the context of the Inglis solution above. Obviously a physical quantity such as the stress cannot really diverge, i.e. there must be some small scale physical regularization of the divergence. However, the square-root singular spatial variation of the stress (and strain) field near the tip of a crack is real and of enormous importance. We already understood that it is this singularity that essentially explains the huge discrepancy between the theoretical and practical strength of materials.

In 1957 Irwin made the next seminal contribution. He pointed out that the series in Eq. (16) is dominated by the $m = -1$ term as the crack tip is approached, $r \to 0$. He therefore focussed on this contribution, for which we have $\lambda = -1/2$ and $b = -a\lambda/(\lambda + 2) = a/3$ in Eq. (9), leading to

$$\sigma_{\theta\theta}(r,\theta) = \frac{a}{4\sqrt{r}} \left[3\cos\left(\frac{\theta}{2}\right) + \cos\left(\frac{3\theta}{2}\right) \right] = \frac{a}{\sqrt{r}} \cos^3\left(\frac{\theta}{2}\right) \; . \qquad (17)$$

Irwin defined $a \equiv K_I/\sqrt{2\pi}$, where K_I is known as the mode I stress intensity factor (the other symmetry modes have their own stress intensity factors). It is a fundamental quantity in the theory of fracture as it quantifies the intensity of the near tip singularity. It has rather strange physical dimensions of stress times square-root of length. Before we continue to discuss it, we note that for $\theta = 0$ we have

$$\sigma_{\theta\theta}(r,0) = \sigma_{yy}(r,0) = \frac{K_I}{\sqrt{2\pi r}} \; , \qquad (18)$$

which directly quantifies the strength of the tensile stress that tends to drive the crack into motion. The other two components of the stress field corresponding to the $m = -1$ term are easily obtained and read

$$\sigma_{r\theta}(r,\theta) = \frac{K_I}{\sqrt{2\pi r}} \cos^2\left(\frac{\theta}{2}\right) \sin\left(\frac{\theta}{2}\right) \; , \qquad (19)$$

$$\sigma_{rr}(r,\theta) = \frac{K_I}{\sqrt{2\pi r}} \cos\left(\frac{\theta}{2}\right) \left[1 + \sin^2\left(\frac{\theta}{2}\right) \right] \; . \qquad (20)$$

This asymptotic stress field $\boldsymbol{\sigma}$ is termed the "K-field".

The emerging mathematical and physical picture is neat. Whatever external geometry and boundary conditions we have, the near crack tip fields are *universal* and characterized by a square-root singularity. All the information about the large scales is transmitted to the crack tip region by a single number, the stress intensity factor K_I – the only non-universal quantity in the universal K-field (if mode II and III loadings are relevant,

we have two additional universal fields, all feature a square-root divergence, and two additional stress intensity factors, K_{II} and K_{III}). As we stressed above, calculating it entails the solution of the global crack problem. In the case of a single straight crack of length ℓ in an infinite medium loaded by a tensile stress σ^∞ at infinity (an Inglis crack), dimensional analysis implies that $K_I \sim \sigma^\infty \sqrt{\ell}$ and only the order unity prefactor should be calculated from the exact global solution.

As we explained above, there must be some physical regularization of the singularity at small scales, which means that nonlinear and dissipative processes (e.g. plasticity) are taking place near the tip of crack relax the stress. Therefore, the K-field should be in fact interpreted as "intermediate asymptotics" separating the large ("outer") scales linear elastic behavior from the small ("inner") scales nonlinear and dissipative behavior. A crucial assumption here is that we indeed have scales separation, i.e. that linear elasticity is valid everywhere except for a region near the crack tip – the so-called "process zone" – whose dimensions are much smaller than any other lengthscale in the crack problem. This assumption is termed "small scale yielding" (though the nonlinear and dissipative processes near the tip are not necessarily or exclusively plastic yielding and deformation). It is important to stress again that the ("inner") scales near the tip of the crack, where fracture is actually taking place, are always subjected to universal boundary conditions in the form of the K-field and that the specific properties of a given problem at the larger ("outer") scales are transmitted to the tip region only through the stress intensity factor. It is this scales separation that makes a linear elastic approach so useful. Fracture is a physical phenomenon that exhibits a rather unique coupling between widely different scales. It is also a natural laboratory for extreme out-of-equilibrium physics that takes place near the tip region even if external loading conditions are mild.

3   Crack tip opening displacement (CTOD)

Let us explore some more consequences of the universal K-field in Eqs. (17), (19) and (20). First, we use Hooke's law to transform this stress field into a displacement field. The result reads (derive)

$$u_x(r,\theta) \;=\; \frac{K_I \sqrt{r}}{4\mu\sqrt{2\pi}} \left[(2\kappa - 1)\cos\left(\frac{\theta}{2}\right) - \cos\left(\frac{3\theta}{2}\right) \right], \qquad (21)$$

$$u_y(r,\theta) \;=\; \frac{K_I \sqrt{r}}{4\mu\sqrt{2\pi}} \left[(2\kappa + 1)\sin\left(\frac{\theta}{2}\right) - \sin\left(\frac{3\theta}{2}\right) \right], \qquad (22)$$

where

$$\kappa = \begin{cases} \dfrac{3 - \nu}{1 + \nu} & \text{for plane-stress} , \\ 3 - 4\nu & \text{for plane-strain} . \end{cases} \qquad (23)$$

We now ask the following question: what is the shape of the crack tip when it opens up under external loadings, i.e. what is the crack tip opening displacement? To answer this question we would be interested in calculating the dependence of $\varphi_x(r,\pi)$ on $\varphi_y(r,\pi)$,
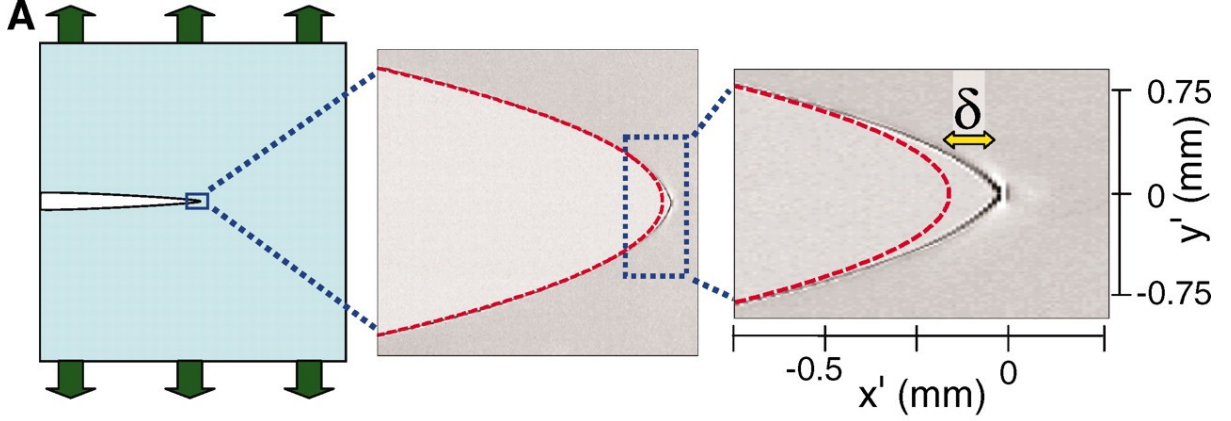
Figure 1: Experimental observation of the CTOD in dynamic fracture. From Livne, Bouchbinder, Svetlizky, & Fineberg, *Science* **327** (2010). Note that at very small scales the CTOD is no longer parabolic, a feature that was used in the paper to study the non-linear corrections to the linear theory of fracture that we're currently discussing. The scale δ is related to the scale where non-linear corrections to the K-field become important.

where $\boldsymbol{\varphi} = \boldsymbol{x} + \boldsymbol{u}$ is the motion (recall that in the linear theory we do not distinguish between the undeformed $\boldsymbol{X}$ and the deformed $\boldsymbol{x}$ coordinates). We then have

$$\varphi_x(r, \pi) = r\cos(\pi) + u_x(r, \pi) = -r \, , \tag{24}$$

$$\varphi_y(r, \pi) = r\sin(\pi) + u_y(r, \pi) \sim \frac{K_I}{\mu}\sqrt{r} \, . \tag{25}$$

Therefore, we obtain

$$\varphi_x(r, \pi) \sim -\frac{\mu^2}{K_I^2}\varphi_y^2(r, \pi) \, , \tag{26}$$

which implies that the crack tip opening displacement is *parabolic*. The curvature of the parabola is determined by μ^2/K_I^2.

4 Example

Consider a finite crack of length $2a$ in an infinite system. The crack occupies the region $-2a < x < 0$ and the system is loaded such that at infinity $\sigma_{yy} \to \sigma_0$ and all other components vanish. This is a pure mode I problem, which is analytically solvable (we solved the analogous mode-III problem, which is considerably simpler, in TA #7). We will not present the full solution here, but just state that the tensile stress along the symmetry axis $y = 0$ is given by

$$\sigma_{yy}(x, 0) = \sigma_0 \frac{x + a}{\sqrt{x}\sqrt{x + 2a}} \, . \tag{27}$$
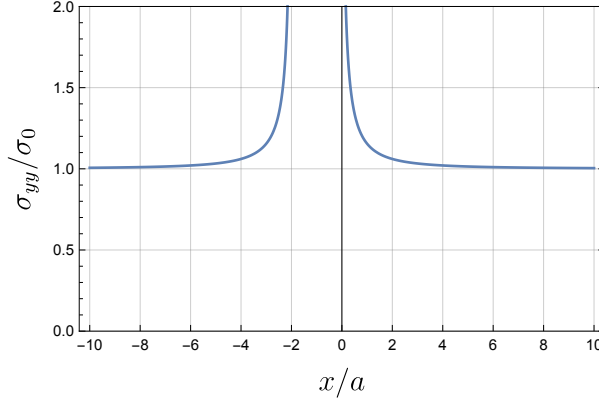
This function is plotted in Fig. 2.

Figure 2: The stress field of Eq. (27)

This is a pretty rare occasion when the full problem is analytically solvable, and not just the intermediate asymptotics between the inner and outer problems, as Eran discussed in class. Let's try to understand what's going on. First of all, note that the stress field is essentially constant for $x > 2a$, i.e. at distances of the order of the crack length. This was a crucial assumption in the scaling theory of fracture, and it is verified here explicitly.

Second, let's see if we can get the Williams expansion around $x = 0$ in this case. The coefficient of the leading singular term, a.k.a the stress intensity factor K_I, can be obtained by

$$K_I = \lim_{x \to 0} \sigma_{yy} \sqrt{2\pi x} = \sigma_0 \sqrt{\pi a} \ . \tag{28}$$

That is, $\sigma = 1/\sqrt{2x} + \mathcal{O}(x^0)$. The next terms in the expansion can be calculated by substituting $\sqrt{x} \to s$ and calculating the Taylor (actually, Laurent) series in terms of s. The result is

$$\sigma_{yy}(x) = \frac{1}{\sqrt{2x}} + \frac{3}{\sqrt{32}} x^{1/2} - \frac{5}{32\sqrt{2}} x^{3/2} + \frac{7}{128\sqrt{2}} x^{5/2} + \mathcal{O}(x^{7/2}) \tag{29}$$

These are plotted in Fig. 3, where it is seen that the K-field gives an essentially perfect description of the total stress field for $x < 0.2$, or $\sigma/\sigma_0 > 3$.

5   Some notes about $x \to 0$

Let's try to see when do we expect the solution to break down at very small x's. Is our solution self consistent and indeed there is an intermediate range where the K-field dominates but linear elasticity still holds?

The solution should break down when linear elasticity breaks down. This might happen due to plastic flow which happens, roughly, when $\sigma \approx \sigma_Y$. At very small x's we are surely inside the K-field, and thus $\sigma \sim K/\sqrt{x}$, i.e. yielding occurs at

$$\sigma_Y \approx \frac{K_I}{\sqrt{x}} \approx \sigma_0 \sqrt{\frac{a}{x}} \qquad \to \qquad x \approx a \left(\frac{\sigma_0}{\sigma_Y} \right)^2 \approx \frac{K_I^2}{\sigma_Y^2} \ . \tag{30}$$
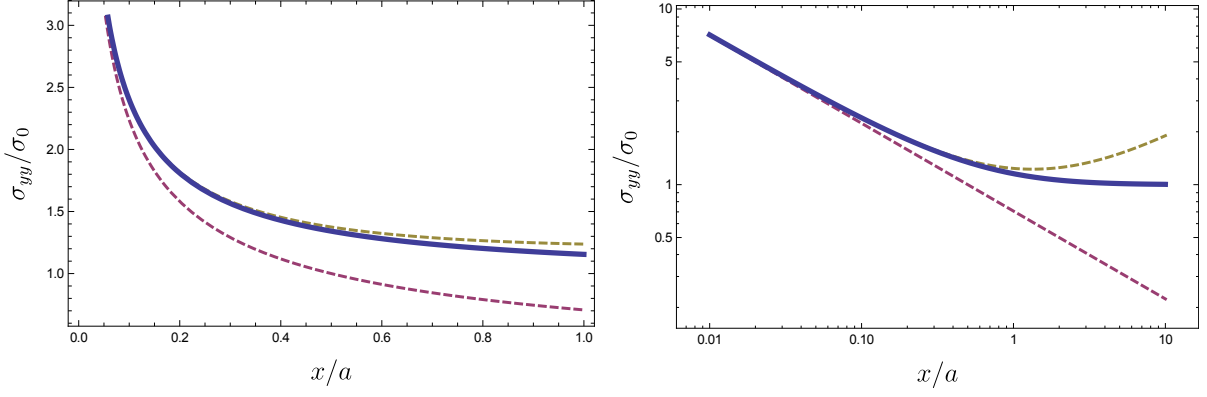
6

Figure 3: The stress field (thick blue), the leading singular term a.k.a the K-field (dashed purple) and the next leading term (dahsed yellow).

Since $\sigma_0 \ll \sigma_Y$, this occurs at x's much smaller than a and the solution is self consistent. Another possibility is that the strain field will deviate towards non-linear elasticity before irreversible flow occurs. This will happen when

$$\epsilon \approx \frac{\sigma}{E} \approx \frac{\sigma_0}{E}\sqrt{\frac{a}{x}} \approx 1 \, , \tag{31}$$

which leads, according to the same scaling, to

$$x \approx a \left(\frac{\sigma_0}{E}\right)^2 \, . \tag{32}$$

Let's try to be a little bit more quantitative about this. Where exactly in space does the material reach the yield criterion? The K field solution is

$$\boldsymbol{\sigma} = \begin{pmatrix} \sigma_{rr} & \sigma_{r\theta} \\ \sigma_{r\theta} & \sigma_{\theta\theta} \end{pmatrix} = \frac{K_I}{\sqrt{2\pi r}} \begin{pmatrix} \cos^3 \frac{\theta}{2} & \cos^2 \frac{\theta}{2}\sin\frac{\theta}{2} \\ \cos^2 \frac{\theta}{2}\sin\frac{\theta}{2} & \cos\frac{\theta}{2}\left(1 + \sin^2 \frac{\theta}{2}\right) \end{pmatrix} \, . \tag{33}$$

We already know that the spatial scale of the plastic zone is $\frac{K_I^2}{\sigma_Y^2}$, and the interesting part is the angular dependence. So let's forget about the prefactor and concentrate on the matrix. It's eigenvalues are

$$\sigma_1 = \cos\frac{\theta}{2} - \frac{\sin\theta}{2} \qquad\qquad \sigma_2 = \cos\frac{\theta}{2} + \frac{\sin\theta}{2} \tag{34}$$

The location of the plastic zone now depends slightly on whether we use plane-stress or plane-strain conditions.

5.1 Plane Stress

For plane stress the third eigenvalue is 0. Therefore, the von-Mises criterion reads

$$\sigma_Y^2 \approx \frac{(\sigma_1 - \sigma_2)^2 + \sigma_1^2 + \sigma_2^2}{6r} = A\frac{7 + 4\cos\theta - 3\cos 2\theta}{24r} \tag{35}$$

7

The Tresca criterion reads

$$\sigma_Y^2 = \frac{A}{r}\frac{1}{4}\max\{(\sigma_1 - \sigma_2)^2, \sigma_1^2, \sigma_2^2\} \ . \tag{36}$$

It can be easily seen that $(\sigma_1 - \sigma_2)^2$ is always smaller than either σ_1^2 or σ_2^2, so this simplifies to

$$\sigma_Y^2 = \frac{\max\{\sigma_1^2, \sigma_2^2\}}{4r} = A\frac{\cos\frac{\theta}{2} + \frac{\sin|\theta|}{2}}{4r} \tag{37}$$

The contour of the elasto-plastic boundary is thus given by

$$r(\theta) \sim \begin{cases} \frac{7 + 4\cos\theta - 3\cos 2\theta}{24} & \text{von-Mises} \\ \frac{\left(\cos\frac{\theta}{2} + \left|\frac{\sin\theta}{2}\right|\right)^2}{4} & \text{Tresca} \end{cases} \tag{38}$$
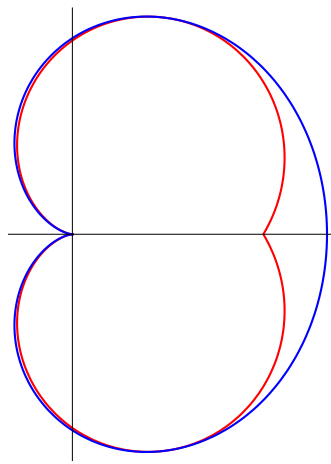
5.2 Plane Strain

For plane strain, we have

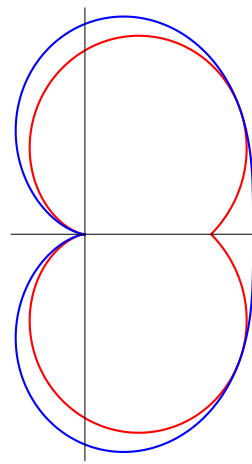$$0 = \epsilon_{zz} = \frac{1}{E}\left(\sigma_{zz} - \nu(\sigma_{xx} + \sigma_{yy})\right) \tag{39}$$

$$\sigma_{zz} = -\nu(\sigma_{xx} + \sigma_{yy}) = -\nu(\sigma_{rr} + \sigma_{\theta\theta}) = -\nu(\sigma_1 + \sigma_1) = -2\nu\cos\frac{\theta}{2} \tag{40}$$

Now you need to divide to cases according to the value of ν, but we won't do that. For $\nu = 1/3$, the results are So we get

$$r(\theta) \sim \begin{cases} \frac{1}{54}\cos^2\frac{\theta}{2}(77 - 27\cos\theta) & \text{von-Mises} \\ \frac{1}{4}\left(\frac{5}{3}\cos\frac{\theta}{2} - \left|\frac{\sin\theta}{2}\right|\right)^2 & \text{Tresca} \end{cases} \tag{41}$$

Plane Strain   Plane Stress

Figure 4: von-Mises (blue) and Tresca (red) elasto-plastic contours for plane stress and plane strain conditions.